ISSN : 0974 - 7486 Volume 8 Issue 11

Trade Science Inc.

Materials Science

An Indian Journal

Full Paper

MSAIJ, 8(11), 2012 [423-433]

Physical study of poly(methyl methacrylate)/rare earth composite luminescent materials

Osiris W.Guirguis[1]*, Wedad A.Alharbi[2], Jamila H.Alzahrani[2]

[1]Biophysics Department, Faculty of Science, Cairo University, Giza, (EGYPT)

[2]Physics Department, Faculty of Sciences for Girls, King Abdul Aziz, (SAUDI ARABIA)

E-mail : osiris_wgr@yahoo.com

Received: 5th April, 2012 ; Accepted: 1st October, 2012

ABSTRACT

In the present work, mixture of five different concentrations (2, 4, 6, 8 and 10 wt%) of an alkali earth aluminate photoluminescent pigment powder (AREAPP) with poly (methyl methacrylate) (PMMA) were prepared. The pigment has the composition formula of $MeO.xAl_2O_3.ySiO_2$:Eu (Me = Ca, Mg, Sr, Ba, x = 0.5-2.0, y = 0.005-0.5) which is activated by rare earth element (Eu). Thermal analyses [differential scanning calorimetry (DSC) and thermogravimetric analysis (TGA)] as well as Fourier transform infrared spectroscopy (FTIR) were employed to characterize and reveal the miscibility map and the relationship of the structure properties. From the results, we can find that the organic parts are attached with the inorganic parts in the PMMA/AREAPP mixtures. Also, the obtained results of the thermal analyses showed variations in the phase transition temperature on the lower temperature side indicating the miscibility of the systems. The changes in the phase transition temperature on the high temperature side, shape and area were attributed to the different degrees of crystallinity.

KEYWORDS

Poly (methyl methacrylate);
Rare earth element;
Luminescent materials;
Structural properties;
Thermal analyses;
FTIR spectroscopy.

INTRODUCTION

Polymer blending provides a powerful route to engineering new properties in materials using available polymers. From polymer blending it is possible to produce a range of materials with properties that are superior to that of each individual component polymers[1,2]. The main advantages of the blended systems are simplicity of preparation and ease of control of physical properties by compositional changes[3] and also it usually requires little or no extra expenditure compared to new polymer synthesis. However, the miscibility between the constituents of polymer mixture on molecular scale is responsible for material with superior properties[4].

Poly (methyl methacrylate) (PMMA) is one of the best organic optical materials and has been widely used to make a variety of optical devices[5], such as optical lenses either in the pure or doped state[6,7], which provides a means to fabricate structures, such as gratings or waveguides.

Poly (methyl methacrylate) has been used in skel-

etal surgery for > 40 years as a means of securing prosthetic implants and more recently was used as a delivery agent for local high-dose antibiotics to treat soft tissue and osseous infections[8]. Moreover, since PMMA is a nondegradable biopolymer, it has been extremely utilized for antibiotic delivery system purposes for the treatment of osteomyelitis[9]. Also, PMMA is a widely used support medium for the embedding of intact, undecalcified bone[10]. Its hardness makes it ideal for calcified tissue sectioning and subsequent histological examination[11].

Luming photoluminescent pigment (has 6 series) is a kind of rare earth photoluminescent powder, with no radioactive component. The photoluminescent pigment powder emits light by absorption of ultraviolet and/or various visible lights in only 15 minutes, then giving out lights for above 12 hours and can be repeatedly used for more than 20 years. The products do not contain any radiating elements, no poisonously, harmlessly.

Luming photoluminescent pigment powder can be used as an additive among the transparent agents. It can be added in coating, ink, paint, plastics, printing paste, ceramics, glass, and fiber etc., to activate the emitting functions of the agents and then the medium can glow in the dark. The products made from the pigment can be safely applied in different fields such as: indication position; safety fields; building; toys; clothing, decorations and others as: arts and crafts, amber, sand crystal, glass, painting works and the systems of transportation, military industry, architecture, etc. Furthermore, some applications of rare earth luminescence are: Lighting technologies, white LED approaches, LED conversion phosphors, persistent phosphors, scintillator phosphors[12]. Applications are numerous in both the commercial and domestic markets.

Some of the first phosphors to be developed were inorganic zinc sulphide compounds. These phosphors typically absorb energy from deep blue and ultraviolet light and emit it as yellow-green light. This is useful in that the peak spectral distribution of the emitted light roughly coincides with the peak spectral sensitivity of the human visual system under isotopic (low-level) lighting conditions (which is around 510 nanometers). Zinc sulphide occurs in crystalline form, but is not photoluminescent by itself. This requires the addition of activator ions to the crystals, such as copper atoms. These ions absorb the excitation energy of the ultraviolet or visible light and later release it as visible light. The copper-activated zinc sulphide crystals (identified with the chemical symbol ZnS:Cu) are typically ground into a fine powder with a grain size of 3 to 15 micrometers to avoid light trapping and light piping effects.

Poly (methyl methacrylate)[13]; oxide glasses[14] are well known as excellent hosts for rare-earth ions. The present phosphorescent pigment (type PLO-6D from six series) used in the present work is a type of long persistence phosphorescent pigment powder of alkaline earth aluminate. The main characteristic of this material is the particular structure of its crystal with the strong capacity of absorbing-storing-emitting light. This luminous pigment is a light-yellow powder which turns to green color after activated by visible light. Compared with the traditional luminous material ZnS, it has the advantages of short activating time, long afterglow time, long lifetime (can be 10 years), high brightness, various environmental adaptation, non-toxic, harmless, non-radioactivity, non-flammability and non-explosive etc. All of these advantages make it sure that the new pigment is an environmental friendly one. It can be easily and widely used in many fields. It has good stability and weather ability. Excitation and emission can be repeated indefinitely.

In the present work, the matrix polymer used is poly (methyl methacrylate) (PMMA). PMMA is mixed with different concentrations (2, 4, 6, 8 and 10 wt%) from an alkali earth aluminate-silicate photoluminescent pigment powder activated by rare earth element (Eu) (AREAPP). Thermal analyses [differential scanning calorimetry (DSC) and thermogravimetric analysis (TGA)] as well as Fourier transform infrared spectroscopy (FTIR) were employed to characterize and reveal the miscibility map and the relationship of the structure properties.

EXPERIMENTAL MATERIALS

Poly (methyl methacrylate) (PMMA) powder CAS:9011-14-7 043982 of chemical formula $[-CH_2C(CH_3)(CO_2CH_3)-]_n$ with average molecular weight of 320,000 and melting point > 150 °C was supplied from Alfa Aesar (A Johnson Matthey Company, Massachusetts, USA). Phosphorescent pigment powder (type

PLO-6D) of alkaline earth aluminate (AREAPP) has a formula: $MeO.xAl_2O_3.ySiO_2$:Eu (Me = Ca, Mg, Sr, Ba, x = 0.5-2.0, y = 0.005-0.5) activated by rare earth element (Eu) was supplied by Dalian Luminglight Science and Technology Co. Ltd., Shanghai, China. Its physical and luminescent properties are given in TABLE 1.

TABLE 1 : Typical physical and luminescent properties of the alkaline earth aluminate phosphorescent pigment powder (AREAPP) used in the present work

Typical physical properties:	
Appearance	yellowish
Density	3.6 g/cm^3
Temperature resistance	250 ^{o}C
Average particle size	10-15 μm
Luminosity life	10 to 20 years depending on manufacturing process, mixing and moisture content of the vehicle
Typical luminescent properties:	
Excitation	UV radiation, white light (any visible light)
Excitation wavelength	200-450 nm
Peak value	520 nm
Glowing color	yellow-green
Brightness of afterglow	> 12 hours after absorbing the light for 10-30 minutes
Temperature resistance	250 ^{o}C

SAMPLE PREPARATION

The PMMA powder is mixed with AREAPP powder for five different concentrations (2, 4, 6, 8 and 10 wt%). The starting materials were ground using a Phillips PW 4018/00 MiniMill for 15 minutes with a rotating speed of 3400 rpm to form a homogenous mixture.

PROPERTY MEASUREMENTS

Thermogravimetric analysis (TGA) and differential scanning calcorimetry (DSC)

Thermal behaviour of the prepared samples was examined by Thermogravimetric Analyzer model Schimadzu TGA-50 (Kyoto, Japan) from 20 to 650 ^{o}C. A heating rate of 10 ^{o}C/min was used under nitrogen atmosphere and at a flow rate of 30 mL/min. The standard uncertainty of the sample mass measurement is ± 1%. Samples were repeated three times to ensure repeatability.

The thermal transition behaviour of the composites was determined by Differential Scanning Calorimeter model Schimadzu DSC-50 (Kyoto, Japan) from 20 to 650 ^{o}C. A heating rate of 10 ^{o}C/min was used under nitrogen atmosphere and at a flow rate of 30 mL/min. Samples were repeated three times to ensure repeatability.

Fourier transform infrared (FTIR)

The IR transmittance spectra of the prepared mixtures over the range 4000-500 cm^{-1} was obtained using potassium bromide pellet technique[15]. The pellets were prepared by mixing 1 mg of powdered sample with 100 mg of dried potassium bromide powder. Mixing was carried out using a pestle and agate mortar. The mixture was then pressed in a special die at a pressure of 10,000 pounds per square inch to yield a disk. The IR spectra of the prepared pellets were then recorded at room temperature by using Perkin-Elmer FTIR Spectrophotometer Model 1650 TX in the wavenumber range from 4000 to 500 cm^{-1} with a resolution of 4 cm^{-1}. The resulting spectra are deconvoluted to enable us to shed further light on the structural changes of PMMA.

Energy dispersive X-ray spectroscopy (EDX)

The elemental analysis of the alkaline earth aluminate phosphorescent pigment powder was done by using Energy Dispersive X-ray Spectroscopy (EDX, Oxford Instruments INCA X-sight) accompanied by the Scanning Electron Microscope (SEM, Jeol JXA 840) operating in liquid nitrogen atmosphere with 5% error (TABLE 2).

RESULTS AND DISCUSSIONS

Thermal gravimetric analysis (TGA)

The thermal degradation kinetics in polymers is more

TABLE 2 : Elemental analysis of the alkaline rare earth aluminate phosphorescent pigment (AREAPP) powder

Element	Mg	Al	Si	P	S	Ca	Ni	Cu	Zn
Weight%	0.449	0.016	7.672	0.881	40.378	0.828	0.017	0.034	49.727

Full Paper

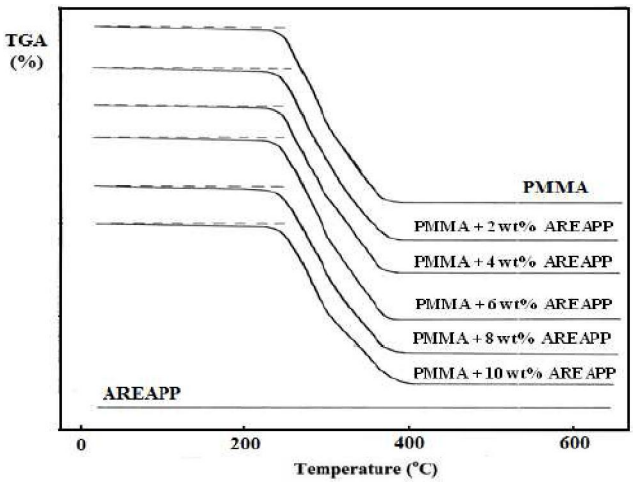

Figure 1 : TGA curves of PMMA/AREAPP composite samples

complicated than in inorganic materials due to the nature of polydispersity of polymer chains. The mechanism of thermal degradation of polymers depends on molecular structure and experimental conditions.

The TGA curves for AREAPP material, pure PMMA and that for PMMA mixed with 2, 4, 6, 8, and 10 wt% AREAPP samples are shown in Figure 1 and the data are given in TABLE 3. It is clear from the figure that, the curves show three weight loss steps and discuss as follows:

Weight loss in the first step which is so slight and assigned to the loss of the moisture of the pure and mixed PMMA samples at about 59.40-77.33 °C, i.e. water vaporization, and the weight loss in this step ranges from 1.283 to 1.832%. The intensity of this peak has close relation to the quantity of water (moisture) in the PMMA samples[16]. As the particle size of the polymer (which refers to the degree of polymerization) decreases the polymer affinity to water increases due to the increasing in its surface area. Beside this peak, a new one is generated due to the glass transition (T_g) occurring in the amorphous regions of the matrix[16]. When adding the AREAPP powder to the PMMA, the particle size changes, so, the crystallinity also changes and then the amorphous regions differ inversely to it, thus, the absorbed heat of glass transition (T_g) also increases. Usually these two peaks combine together to produce one peak (peak 1 in the DSC curves, as shown in Figure 3). The observed variation in T_g points to a variation in the inter-particle distances and interface interactions. The increase in the glass transition temperatures of the mixed PMMA samples compared to that of pure PMMA (TABLE 3) by increasing the percentage content of AREAPP, can be explained that the motion of PMMA chains in restricted by this mixing.

The major decomposition step which is attributed to PMMA polymer decomposition into small molecules such as: CO_2, H_2O and others flammable substances of PMMA and of the added AREAPP. The temperature at which this second step of loss occurred is at about 296-302 °C and the weight loss ranges from 90 to 98%. From Figure 1, a dramatic drop in weight is observed for the second loss stage. The pure PMMA sample looses 98.12% of its weight at 296.5 °C with a residual weight of 0.168%. This weight loss is attributed to the degradation of unsaturated groups of PMMA as proven in DSC diagram (Figure 3). It is observed that the mixing of PMMA with AREAPPP enhances the thermal stability at higher decomposition temperature. This second significant weight loss may be due to the unzipping process which contributes to a reduction in molecular weight of polymer chains at high temperatures. This unzipping reaction induces many degradation reactions such as random chain scissions, depolymerization, inter- and intra-molecular transfer reactions whereby dimmers, trimmers and oligomers are pro-

TABLE 3 : TGA and DrTGA data for PMMA/AREAPP composite samples

Composite samples	First step		Second step		Third step		Residue %
	% weight loss	Mid point (°C)	% weight loss	Mid point (°C)	% weight loss	Mid point (°C)	
PMMA	1.832	59.40	98.120	296.51	0.168	393.00	0.000
PMMA + 2 wt% AREAPP	1.561	66.07	96.570	299.04	0.217	408.12	1.625
PMMA + 4 wt% AREAPP	1.283	69.13	94.240	297.97	0.239	395.03	4,238
PMMA + 6 wt% AREAPP	1.647	60.22	93.475	302.65	0.188	475.22	4.760
PMMA + 8 wt% AREAPP	1.733	77.33	93.240	301.72	0.972	487.60	5.055
PMMA + 10 wt% AREAPP	1.550	71.40	90.070	296.45	0.525	409.49	7.855

duced as well as fragments[17]. As a result, the monomers and oligomers which adsorbed onto the polymer matrix are volatilized in this stage. The degradation of PMMA in this region follows a two–step process. The first process, endothermic centered at 296.5 °C, due to the degradation of unsaturated chains ends and the second one at 393 °C which is attributed to random scission of the polymer chains[18].

Moreover, the first endothermic peak is weaker than the second one in pure PMMA sample and differs greatly in case of mixed PMMA samples with different concentrations of AREAPP. The temperature of the first endothermic peak increased by about 6.67, 9.73, 5.82, 17.93 and 12.00 °C, respectively, for PMMA mixed with 2, 4, 6, 8 and 10 wt% of AREAPP samples. The temperature of the second endothermic peak increased by about 2.53, 1.46, 6.14 and 5.21 °C, respectively, by increasing the wt% of AREAPP up to 8wt% (TABLE 3).

The weight loss of the third step is mainly caused by the char decomposition and oxidation of PMMA polymer. The remarkable difference in TG curves between the pure PMMA and its mixed samples with AREAPP in different weight percent were in the initial decomposition temperatures and char residue (TABLE 3). While, the char residue weight is given by:

$$\text{Char residue weight} = W_1 - W_2 \quad (1)$$

Where W_1 is the total sample weight and W_2 is the weight loss after total sample decomposition.

So, the production of more char (less in weight loss during the composition) in case of PMMA mixed with rare earth metal at concentration of 10 wt% means that thermal stability of this sample is enhanced and it is more resistant to fire hazards. When the temperature rises above 300 °C; slight final loss occurs, this is caused by the chemical groups in the crystalline regions of the polymer. Therefore, following the rise in temperature, PMMA polymer first decomposes in the amorphous region, and then in the crystalline region[19]. Thermal degradation of PMMA sequently occurs as initial scission, depropagation reactions and further degradation into volatile compounds[20].

At least two mechanisms have been validated for the initial scission of PMMA, including random scission (C-C bonds) of the main chain and hemolytic scission of the methoxycarbonyl side groups (-$COOCH_3$). The random C-C scission is the dominant mechanism, which decomposes PMMA into methyl methacrylate as a major product[21]. However, the products such as CO_2, CO, CH_3OH, CH_4 and char, other than the monomer could also form along with the elimination of methoxycarbonyl side groups[22]. The kinetics of PMMA decomposition was investigated as a first order reaction for most previous studies.

PMMA ignites at 460 °C and burns forming carbon dioxide, water, carbon monoxide and low molecular weight compounds, including formaldehyde. By following the temperature of the third endothermic peak listed in TABLE 3, it is noticed that it increases for PMMA samples mixed with increasing the wt% of AREAPP. This may be attributed to that as the content of AREAPP increases in the PMMA polymer; the composites became more thermally stable which indicate better dispersed of AREAPP in PMMA matrix.

Differential thermogravimety (DrTGA)

Differential thermogravimety (DrTGA) results of pure PMMA and those of mixed PMMA with different concentrations of AREAPP are shown in Figure 2 and are listed in TABLE 3. From TABLE 3, the values of the decomposition temperatures for all the samples are detected. These decompositions depend upon the molecular weight and the purity of the polymer, i.e., PMMA in this case, and are affected by its morphology. The first endothermic peak of the blank PMMA at about 59.40 °C is corresponding to the total moisture loss. For all mixed PMMA samples, this endothermic peak lies between 59.40 and 77.33 °C. The second endothermic peak for pure PMMA is detected at about 296.51 °C which reflects the decomposed reaction of PMMA. The values of the second endothermic peak shifted toward higher temperatures by increasing the contents of AREAPP from 296.51 up to 302.65 °C and shows wide right shoulder as in the case of pure PMMA. This shoulder differs in depth according to the percentage content of AREAPP and it is shallow in case of 2 and 10 wt% of AREAPP. There are many shoulders seen in the left side of this peak, which may be attributed to the presence of metals in the AREAPP which have low decomposition temperatures such as phosphorous and sulpher (melting points 44.1 and 112.8

Full Paper

°C, respectively). The appearance of the shoulder means that the average side of crystallites is changed due to the adding of AREAPP to PMMA polymer.

Heat release during the decomposition is represented by the area under the third endothermic peak. It has the highest value (487.60 °C) for PMMA polymer mixed with 8 wt% of AREAPP, while the lowest one (395.03 °C) is that for PMMA mixed with 4 wt% AREAPP (TABLE 3). The small peaks appeared in the end of the temperature curves for all samples are assigned to the heat released of oxidation of the decomposition of flammable products of the samples.

Differential scanning calorimetry (DSC)

Figure 3 shows DCS curves for the pure and mixed

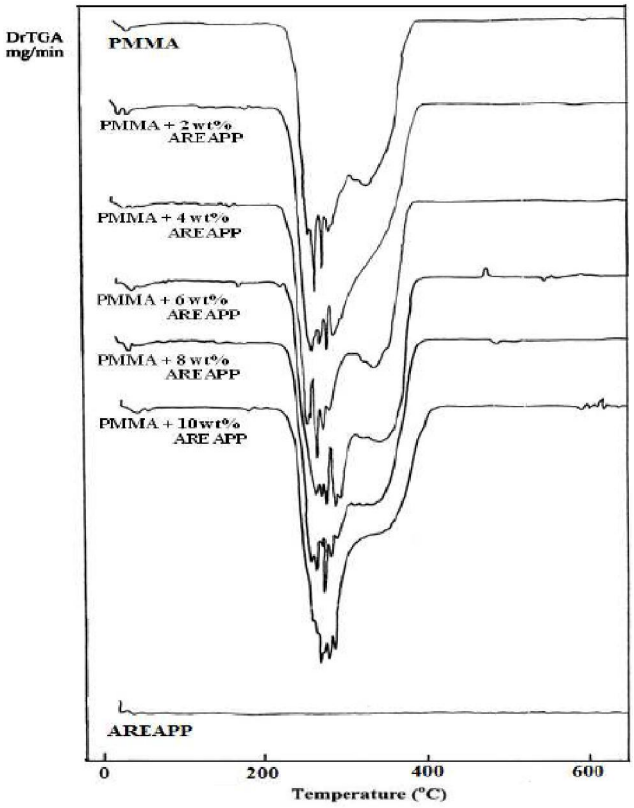

Figure 2 : DrTGA curves of PMMA/AREAPP composite samples

PMMA samples with different concentrations of AREAPP. The measurements from the DSC curves are tabulated in TABLE 4. Difference in shape and area of the decomposition endothermic were noticed.

The different in shape can be attributed to the different degree of crystallinity found in the different PMMA investigated samples[23]. Peaks broadened as O-H content declined. The hydroxyl groups are highly interconnected by hydrogen bonding, leads to higher glass transition temperature (T_g). The introduction of other functional groups (as earth metal groups in our case) may

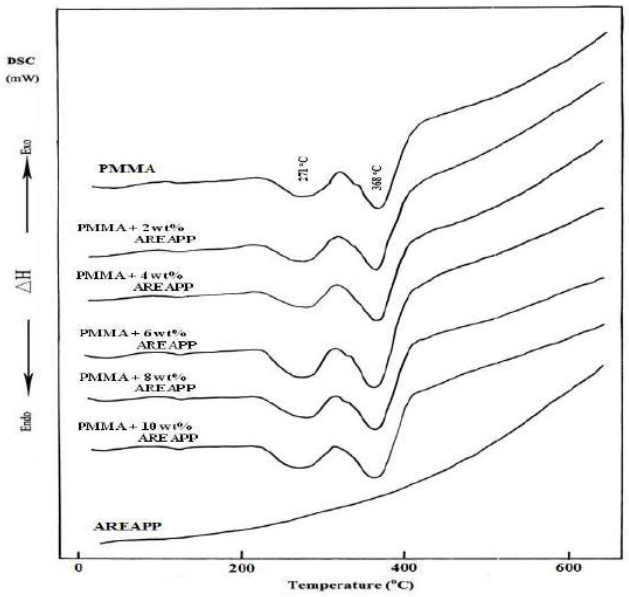

Figure 3 : DSC curves of PMMA/AREAPP composite samples

support this bonding and enhance the T_g value. Also, a reduction in the peak area indicated a change in the extent of crystallinity or in molecules order[24]. On the other hand, a decrease in enthalpy of fusion and increase in melting temperature suggested that the crystallinity and perfection of the crystal structure were reduced by increasing the degree of cross-linking. Change in the crystalline structure can results from PMMA polymer and earth metals molecules interactions in the amorphous phase of PMMA polymer. So, disorder in the crystals is created, reducing the enthalpy of the phase change[25,26].

From Figure 3 and TABLE 4, the major endothermic peak is observed at 270.98 °C corresponding to the decomposition temperature of the blank PMMA sample. For the other PMMA polymer mixed with AREAPP, the decomposition endotherm was slightly broadened and the peak temperature shifts towards higher values with increasing the concentration of AREAPP.

Fourier transform infrared (FTIR) spectral analysis

FTIR spectroscopy has long been recognized as a powerful tool for elucidation of structural information.

TABLE 4 : Values of transition temperatures and associated heat of fusion for PMMA/AREAPP composite samples

Composite samples	Second step				Third step		
	Onset temp. (°C)	Peak temp. (°C)	Endset temp. (°C)	Heat release (J/g)	Peak temp. (°C)	Endset temp. (°C)	Heat release (kJ/g)
PMMA	236.82	270.98	313.91	-101.60	367.60	421.69	-2.21
PMMA + 2 wt% AREAPP	327.52	366.95	406.26	-302.91	366.95	424.13	-2.89
PMMA + 4 wt% AREAPP	234.33	282.00	310.06	-79.92	367.95	429.66	-2.51
PMMA + 6 wt% AREAPP	232.88	281.91	315.14	-138.00	367.80	417.04	-2.09
PMMA + 8 wt% AREAPP	284.78	367.68	408.58	-732.70	367.68	417.04	-2/19
PMMA + 10 wt% AREAPP	308.15	367.98	409.19	-722.91	367.98	418.80	-2.15

The position, intensity, and shape of vibrational bands are useful in clarifying conformational and environmental changes of polymers at the molecular level. The FTIR spectra of PMMA, AREAPP and their mixtures in the frequency range 4000-500 cm^{-1} are shown in Figure 4, in transmission mode.

The FTIR spectrum of PMMA indicates the details of functional groups present in the synthesized PMMA and is comparable to that of earlier reports[2,13,27-30]. It is clear from the figure, absorption that arises from C-H stretching of the methyl groups occurs in the region of 3000-2840 cm^{-1}, which contain two distinct peaks at 2997 and 2946 cm^{-1} resulting from asymmetrical and symmetrical stretching modes of C-H bonding in the methyl group, respectively. Also, the distinct band appeared at 2853 cm^{-1} arises from the C–H bond vibration of the methyl group. The peak in the region 1750-1730 cm^{-1} represents C=O double bond stretching vibration of the aliphatic esters. Symmetrical bending vibration occurs near 1392 cm^{-1} (δ_s CH_3), while the asymmetrical bending vibration (δ_{as} CH_3) of methyl group is identified near 1494 cm^{-1}. The band at 1632 cm^{-1} corresponds to the C=O stretching ester group, also, it may appear from deformative water molecules which is probably due to water absorption during the compaction of the powder specimens with KBr[31]. The bands at 1278 cm^{-1} is associated with C-O stretching vibration. The bands at 1130 and 1064 cm^{-1} are attributed to asymmetric and symmetric stretching vibration of C–C groups, respectively. The bands at 987 and 749 cm^{-1} arise from the aliphatic –CH_2 group. The band at 912 cm^{-1} is related to syndiotactic structure and is assigned to the δ_r (CH_2) rocking vibration. The bands at 841 cm^{-1} is assigned to -CH_2 rocking vibration group, while the band at 650 cm^{-1} is due to the bending of C-H mode.

Also, from Figure 4 it is shown that, the FTIR spectrum of AREAPP sample indicates the details of functional groups present and is comparable to that of earlier report[32]. This spectrum exhibits broad band near 3469 cm^{-1} due to the OH-stretching vibrations of free and hydrogen-bonded hydroxyl groups. On other hand, the band in the region 3750-3300 and at 1632 cm^{-1} are most probably due to the humidity absorbed by the KBr during the preapartion of the pellets (i.e., O-H group). The appearance of a band at 1494 cm^{-1} is due to the asymmetrical bending vibration (δ_{as} CH_3) of methyl group. The band at about 1097 cm^{-1} is assigned to δ (C-O) stretching vibration of ether group. The metal–oxygen stretching frequencies in the range 1000–500 cm^{-1} are associated with the vibrations of metals-oxygen, e.g., Al–O, Si–O and Si–O–Al bonds and AlO_4 unit[33].

From the obtained results of the PMMA/AREAPP composite samples shown in Figure 4 it is clear that: The band of the methoxy carbon (O–CH_3) which appeared at 2853 cm^{-1} has shifted to a higher value with increasing the weight percent of AREAPP. Pronounced shift to lower values was detected in the carbonyl band for PMMA sample at 1744 cm^{-1} which is an evidence of side group elimination from PMMA chains upon increasing the concentration of AREAPP. In addition, the shift detected of the carbonyl band from 1744 to 1727 cm^{-1} indicated a change in the balance of free and associated carbonyl groups in the compositions. The wavenumbers corresponding to the characteristic transmission peaks of PMMA as asymmetrical and symmetric bending vibration (δ_{as} CH_3 and δ_s CH_3) of methyl groups at 1494 and 1392 cm^{-1}, respectively, have not been affected by increasing the concentration of AREAPP. Similarly, the band at 1632 cm^{-1} which corresponds to the C=O stretching ester group and the band

Full Paper

841 cm^{-1} assigned to CH_2 rocking, show nearly unremarkable shift in their positions.

The heights of the peaks of the assigned groups at their wavenumbers shown in the spectra were taken to represent the variation in the group band intensities for different AREAPP concentrations (Figure 5). A clear deviation was observed in the transmittance bands of the PMMA/AREAPP composites when compared with that detected for pure PMMA. The increase and/or

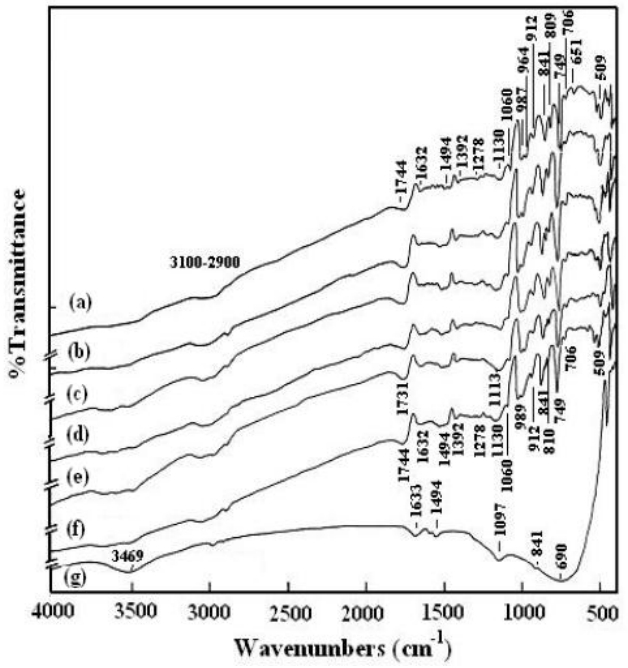

Figure 4 : Variations in FTIR spectra of PMMA/AREAPP composite samples. (a) Pure PMMA, (b) PMMA + 2 wt% AREAPP, (c) PMMA + 4 wt% AREAPP, (d) PMMA + 6 wt% AREAPP, (e) PMMA + 8 wt% AREAPP, (f) PMMA + 10 wt% AREAPP, and (g) Pure AREAPP

decrease in the intensity mean that there is a change in the molecular configuration of the polymer network.

As shown by the FTIR results, it was clear that an increase in the concentration of AREAPP changed the chemical bonds and hence changed the molecular configuration of PMMA which is shown by the pronounced variation in the intensity of transmittance bands and shifts in band positions. The change in intensity of some spectral bands associated with infrared active groups of PMMA and AREAPP may be attributed to the fact that in the materials that contain two or more components, the resulting spectrum is approximately the sum of their components. In addition, the change in the spectral position of some bands of PMMA after the additions of

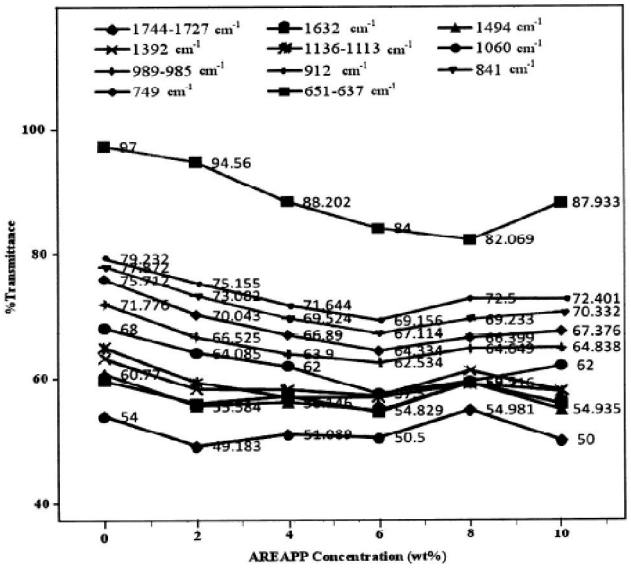

Figure 5 : Variations in band intensities for some chemical groups of PMMA/AREAPP composite samples

different AREAPP concentrations may be attributed to some of the monomer units of PMMA are sensitive to their environment. Furthermore, the hydroxyl and carbonyl stretching vibration bands are affected by hydrogen bonding interactions and are most amenable to

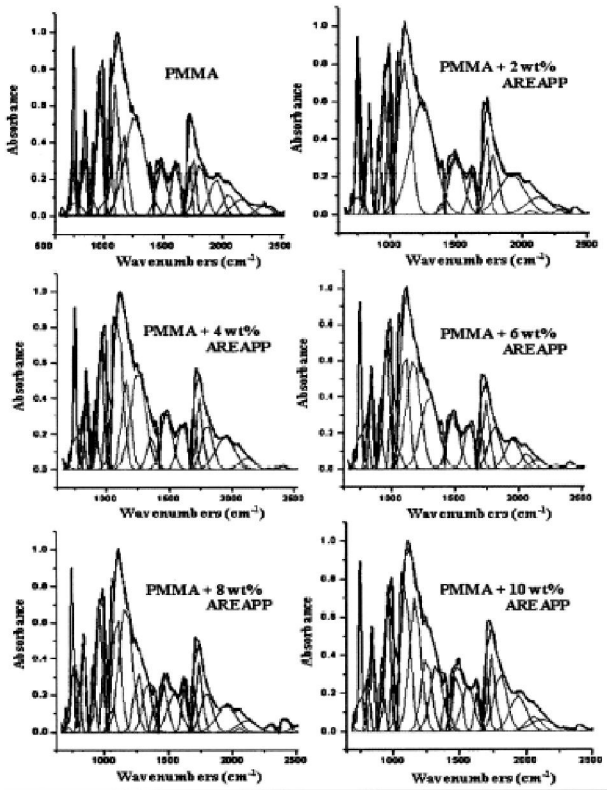

Figure 6 : Band deconvolutions of IR spectra for PMMA/AREAPP composite samples. The red line shows the fit of the IR spectra

TABLE 5 : Deconvolution parameters of the infrared spectra of PMMA/AREAPP composite samples

Parameters	PMMA + AREAPP (wt%)					
	PMMA	2 wt%	4 wt%	6 wt%	8 wt%	10 wt%
Band position (cm^{-1})	750.84	751.11	750.83	751.13	750.73	751.02
Band width (cm^{-1})	18.94	19.00	21.53	21.64	21.82	21.24
Area under the peak	19.80	19.90	23.73	24.24	23.78	22.88
Band position (cm^{-1})	838.50	841.38	841.45	841.99	841.75	841.86
Band width (cm^{-1})	34.69	26.78	25.65	25.90	25.33	25.78
Area under the peak	20.25	18.78	17.28	17.72	16.41	17.10
Band position (cm^{-1})	911.53	913.29	912.54	911.29	911.33	912.92
Band width (cm^{-1})	22.53	25.94	25.44	23.04	22.72	25.81
Area under the peak	9.70	12.03	11.14	9.70	9.18	11.30
Band position (cm^{-1})	962.69	960.85	961.45	962.77	962.53	961.69
Band width (cm^{-1})	43.39	36.34	38.80	43.66	42.24	37.77
Area under the peak	42.84	36.04	37.67	42.01	38.63	36.21
Band position (cm^{-1})	994.26	992.23	992.92	994.25	993.95	993.20
Band width (cm^{-1})	18.88	18.87	18.59	18.76	19.32	19.00
Area under the peak	13.66	15.53	14.25	13.28	13.44	14.83
Band position (cm^{-1})	1058.39			1058.37	1057.69	
Band width (cm^{-1})	23.77			21.243	22.38	
Area under the peak	16.12			12.99	13.89	
Band position (cm^{-1})	1102.35	1105.28	1092.57	1101.75	1098.94	1089.24
Band width (cm^{-1})	58.26	94.14	75.44	64.15	58.71	70.68
Area under the peak	55.63	97.21	85.59	56.86	52.43	72.14
Band position (cm^{-1})	1161.85	1194.68	1161.25	1170.93	1168.05	1164.32
Band width (cm^{-1})	74.77	0.07	70.86	108.72	98.04	84.20
Area under the peak	42.17	11.08	44.72	83.45	86.25	75.00
Band position (cm^{-1})	1263.19	1240.72	1255.40	1261.78	1263.97	1250.07
Band width (cm^{-1})	172.12	180.21	117.77	0.245	65.16	77.05
Area under the peak	116.30	135.96	82.35	22.00	26.62	38.43
Band position (cm^{-1})	1487.07	1500.31	1480.49	1486.26	1465.28	1482.38
Band width (cm^{-1})	87.64	105.73	86.74	86.65	56.24	51.96
Area under the peak	30.89	41.89	36.22	33.27	18.43	21.26
Band position (cm^{-1})	1607.16	1617.13	1605.65	1608.62	1628.60	1629.16
Band width (cm^{-1})	69.52	53.72	74.37	71.54	39.69	36.59
Area under the peak	25.30	15.36	25.14	23.53	12.46	9.36
Band position (cm^{-1})	1711.67	1720.88	1709.48	1710.05	1707.23	1709.69
Band width (cm^{-1})	28.19	44.79	25.96	25.38	24.56	27.30
Area under the peak	13.54	26.89	12.00	10.13	9.62	12.23
Band position (cm^{-1})	1747.23	1776.89	1742.55	1743.79	1738.91	1742.69
Band width (cm^{-1})	49.82	79.86	47.93	53.50	48.13	51.25
Area under the peak	23.25	32.07	24.22	25.50	23.09	25.89

quantitative analysis.

The relative area of the deconvoluted bands in the region (1800–700 cm^{-1}) indicates the variation in the structure, so that, as the AREAPP content increases the area of these bands change. Furthermore, each individual band has its characteristic parameters such as

its centered band position which is related to some type of vibration of a specific structural group, and its band width which is proportional to the concentration of this structural group. A Gaussian deconvolution process should be performed to get such parameters (Figure 6 and TABLE 5).

From Gaussian deconvolution of the IR spectra, it is clear that, principal broad bands at around 1100, 1487, 1607 and 1750 cm^{-1} are present. Little change in the centre of the bands around 1100 and 1487 cm^{-1}, while the centre of the band around 1607 cm^{-1} shifts to higher wavenumber; the centre of the band around 1750 cm^{-1} shifts to a lower wavenumber and their width become wider as the AREAPP content increase from 2 up to 10 wt%. The area and the band width of the bands at 839, 963, 1263, 1487 and 1607 cm^{-1} showed decrease, while the bands at 751 and 1162 cm^{-1} showed increase in their area and band width with increasing AREAPP concentration. On other hand, approximately, wavy variation in the area and band width of the bands at 963, 994, 1102, 1711 and 1747 cm^{-1} is observed with increasing the concentration of AREAPP.

CONCLUSION

Thermal analysis technique is a very accurate tool to differentiate between the thermal stability of PMMA polymer sample before and after mixing with different weight% of alkali earth aluminate photoluminescent pigment powder (AREAPP), and to understand the mechanism of mixing. TGA and DSC analyses showed that the mechanism of mixing PMMA polymer with 2, 4, 6, 8 and 10 wt% of AREAPP converts the PMMA polymer to carbonaceous residue or char when exposed to high temperature and hence reduce the volatile formation.

The improvement in thermal stability of PMMA polymer is ascribed to both the good thermal stability of the added AREAPP chemical groups on the particle surface and internal pore channel surface. Moreover, the increase in char yield with the increase of weight percentage of added AREAPP may be because PMMA main chains on the surface and inside the pores are more difficult to decompose than the pure PMMA. This indicates that the metals dispersion in PMMA matrix was uniform and thus hindered the segmental motion of PMMA chains.

There is a relation between the changes in the chemical group coordination in the infrared regions and the percentage of weight mixing of AREAPP with PMMA polymer and the way in which it interact with the PMMA polymer chemical groups. The variation in absorption with the change of percentage mixing may be due to the change in the molecular configuration as a result of the change in the chemical bonds in the PMMA sample and the rare earth metals.

ACKNOWLEDGEMENT

The authors would like to thank Mr. Fouad R.Amal for supporting the AREAPP material.

REFERENCES

[1] A.M.Stephen, T.P.Kumar, N.G.Renganathan, S.Pitchumani, R.Thirunakaran, N.Muniyandi; J. Power Sources, **89**, 80 **(2000)**.
[2] M.S.Khan, R.A.Qazi, M.S.Wahid; AJPAC **2**, 41 **(2008)**.
[3] A.M.Rocco, R.P.Pereira, M.I.Felisberti; Polymer, **42**, 5199 **(2001)**.
[4] A.V.Rajulu, R.L.Reddy, S.M.Raghavendra, S.A. Ahmed; Eur.Polym.J., **35**, 1183 **(1999)**.
[5] R.M.Ahmed; Int.J.Polym.Mater., **57**, 969 **(2008)**.
[6] C.Wochnowski, S.Metev, G.Sepold; Appl.Surf.Sci., **706**, 154-155 **(2000)**.
[7] T.Kardinahl, H.Franke; Appl.Phys.A., **61**, 23 **(1995)**.
[8] V.L.Schade, T.S.Roukis; J.Foot Ankle Surg., **49**, 55 **(2010)**.
[9] S.P.Mohanty, M.N.Kumar, N.S.Murthy; J.Orthop. Surg., **11**, 73 **(2003)**.
[10] N.L.Pleshko, A.L.Boskey, R.Mendelsohn; J. Histochem.Cytochem., **40**, 143 **(1992)**.
[11] A.Stevens, J.Germain; 'Resin embedding media', J.D.Bancroft, A.Stevens, (Eds); The Theory and practice of histological techniques, New York, Churchill Livingstone, **3**, **(1990)**.
[12] M.J.Weber; 'Scintillator materials for calorimetry', Proceedings of the V international conference on calorimetry in high energy physics, **(1994)**.
[13] L.Peng, Y.Luo, Y.Dan, L.Zhang, Q.Zhang, S.Xia, X.Zhang; Colloid.Polym.Sci., **285**, 153 **(2006)**.
[14] G.C.Righini, M.Ferrari; Riv.Nuovo.Cimento., **28**, 1 **(2006)**.

[15] V.Sankar, T.Suresh Kumar, K.Panduranga Rao; Trends in biomaterials and artificial organs, **17**, 24 **(2004)**.
[16] X.Weilin, G.Weigi, L.Wenbin; J.Appl.Polym.Sci., **87**, 2372 **(2003)**.
[17] Z.Ahmed, N.A.Al-Awadi, F.Al-Sagheer; Polym. Degrad.Stabil., **92**, 1025 **(2007)**.
[18] W.Li, M.Yuan, M.Yang; Eur.Polym.J., **42**, 1396 **(2006)**.
[19] K.Hirabayashi; 'Silk physics', Society of silk science and technology in tokyo university of agriculture and technology, Tokyo, **(1980)**.
[20] G.Madras, J.M.Smith, B.J.McCoy; Ind.Eng.Chem. Res., **35**, 1795 **(1996)**.
[21] M.C.Costoche, D.Wang, M.J.Heidecker, E.Manias, C.A.Wilkie; Polymers for advanced technologies, **17**, 272 **(2006)**.
[22] B.J.Holland, J.N.Hay; Polymer, **42**, 4825 **(2001)**.
[23] R.Gireco; 'Polymer blends and mixtures', D.J.Walsh, J.S.Higgins, A.Maconnnachie, (Eds); NATOASI Series E., Applied Science, Nijhholl, The Hague, The Netherlands, **89**, **(1985)**.
[24] S.L.Ciemniecki, W.G.Glasser; Polymer, **29**, 1030 **(1988)**.
[25] R.Hammel, W.J.MacKnight, F.E.Karasz; J.Appl. Phys., **46**, 4199 **(1975)**.
[26] W.Wenig, F.E.Karasz, W.J.MacKnight; J.Appl. Phys., **46**, 4166 **(1975)**.
[27] A.Sar, C.Alkan, A.Karaipekli; Applied Energy, **87**, 1529 **(2010)**.
[28] O.H.Kim, K.Lee, K.Kim, B.H.Lee, S.Choe; Polymer, **47**, 1953 **(2006)**.
[29] D.Saikia, A.Kumar; Eur.Polym.J., **41**, 563 **(2005)**.
[30] A.Balamurugan, S.Kannan, V.Selvaraj, S.Rajeswari; Trends in biomaterials and artificial organs, **18**, 41 **(2004)**.
[31] D.Dvoranova, V.Nrezova, M.Mazur, M.A.Malati; Appl.Catal.B: Environ., **37**, 91 **(2002)**.
[32] V.Singh, J.J.Zhu, M.Tiwari, M.Soni, M.Aynayas, S.H.Hyun, R.Narayanan, M.Mohapatra, V.Natarajan; J.Non-Cryst.Solids, **355**, 2491 **(2009)**.
[33] S.Angappan, J.L.Berchmans, C.O.Augustin; Mater.Lett., **58**, 2283 **(2004)**.